International Journal of Advances in Applied Sciences (IJAAS)
Vol. 11, No. 3, September 2022, pp. 232~241
ISSN: 2252-8814, DOI: 10.11591/ijaas.v11.i3.pp232-241

Skin cancers image classification using transformation and first order statistic features with artificial neural network classifier

Asmaa Abdulrazaq Alqaisi[1], Loay Edwar George[2]
[1]Department of Computer Science, College of Education for Women, University of Baghdad, Baghdad, Iraq
[2]University of Information Technology and Communication, Baghdad, Iraq

Article Info

Article history:

Received Feb 21, 2022
Revised Jun 27, 2022
Accepted Jul 16, 2022

Keywords:

Color image feature extraction
Deep learning
Discrete cosine transform
Discrete wavelet transform
Skin cancer classification
Statistical methods

ABSTRACT

Skin cancer is one of the most dangerous types of cancer. Some types of this cancer lead to death, so cancer must be discovered and indexed to avoid its spread through initial detection in the impulsive stage. This paper deals with the detection and indexing of different types of melanomas using an artificial neural network (ANN) depending on the international skin imaging collaboration (ISIC) 2018 dataset that was used. The pre-processing is the most important part because it formulates an image by insolated the cancer part from the skin image. It consists of four stages, removable, cropping, thinning, and normalization. This phase has been used to eliminate all the undesirable hair particles on the image lesion. The cropped image transforms into frequency domain coefficients using discrete cosine transform (DCT), discrete wavelet transform (DWT), and gradient transform for sub-band images to extract its feature. The statistical feature extraction is implemented to minimize the size of data for ANN training. The experimental analysis used dataset ISIC 2018 consisting of seven different types of dermoscopic images (this paper deals with four types only). For classification purposes, ANN was implemented and the accuracy obtained is about 88.98% for DWT, 85.44% for sub-band DCT, and 76.07% for sub-band gradient transform.

Corresponding Author:

Asmaa Abdulrazaq Alqaisi
Department of Computer Science, College of Education for Women, University of Baghdad
Al-Jadriya, Karrada, Baghdad, Iraq
Email: asma_72@coeduw.uobaghdad.edu.iq

1. INTRODUCTION

Skin cancer is the most common cancer worldwide, known for its increasing incidence rates and increasing burden, it is also difficult to visually distinguish normal tumors from abnormal and general tumors. General practitioners (GPs) usually do not have sufficient experience to diagnose skin cancers [1]. That's why the search focuses on the development and implementation of skin cancer systems to improve the quality of diagnostics by using three-technique with first-order statistical features to detect border of lesions followed by feature extraction selection and classification.

Uninhibited development of irregular skin cells is acknowledged as a skin tumor. It happens when deoxyribonucleic acid (DNA) damage to skin cells generates changes, or genetic faults, that principal the skin cells to multiply quickly and form menacing cancers. Skin cancers have usually diagnosed by physical analysis and surgery [2]. The surgery is a simple way where part or all of the spot is removed and tried in the test center. The dermoscopy is the most effective method to generate color skin imaging, which is the most improved tool in the analysis of tumors depending on the experiment doctor's eye [3]. The standard datasets

of skin cancer are limited and cover a few numbers of skin cancer types, with a little number of images for every type [4].

New methods for skin cancer classification are the goal of researchers works are related to perfect methods of cancer classification. Work on skin image data replicated by flipping and rotation compensates for variations between the training and the test sets and has an optimistic effect on the convolutional neural network (CNN) presentation [5]. Used neural network (NN) to categorize skin cancer into three kinds. The type of dermoscopic images has been implemented in this work, which directly works on color images of skin without pre-processing [6]. Uses an extra dense NN and tempers the features with the CNN [7]. This work attainment to explain the dataset method by counting outside data with skin lesions category. The other class lesion problem is the severe class imbalance number of images. This paper care of this property by considering die rent method input resolutions and die rent cropping stratagems, by integrating data depending on age, structural site, and sex. Classified three-dimensional (3D) image shapes were performed by converting them to images of two-level (binary 0 and 1) [8]. The new algorithm called adaptive snake used to extract the segment features and classification by artificial neural network (ANN) has been employed.

The ANN model was built to produce abstractions accuracy in data using multiple dispensation layers. The important elements of using ANN are: i) The minimizing of cancer huge data for the training and NN models; ii) Graphic processing unit was developed to depiction for computer analysis; and iii) The linear unit, dropout, and batch normalization has been corrected in ANN methods [9]. The automatic identification of tumors from dermoscopy color images has three interesting contracts. First, the skin is very like lesions typical belongs to different lessons, such as size, texture, color, and shape. Second, is the high association between melanoma and non-melanoma lesions. Third, different environmental conditions, such as hair, veins, noise, and radiance [10]–[12].

In this work different types of feature extraction with first-order statistic calculation for pre-processing, the image has been applied to the ANN to classify the skin cancer types and reach to accurate diagnosis of classification. In this work, two cascade feature extraction methods have been used. First, is the transformer method, discrete cosine transform (DCT), discrete wavelet transform (DWT), and gradient method has been used. Second is the statistical methods, which calculate mean, standard deviation, skewness, and the fourth momentum has been implemented to minimize the data and extract features. The ANN has been used to identify and classify cancer types.

2. DISCRETE WAVELET TRANSFORM (DWT)

The wavelet transform converts the image pixels from the space domain to the frequency domain (DWT coefficients). It includes a cluster of low pass filters and high pass filters named filter bands. In DWT may filter can use to generate multi-level DWT. The DWT uses filter bands to take away divisions of the pixels into many frequency bands. The DWT translates the pixels into multi-scale depictions of both spatial and frequency selves to gather. These tips are for effective multi-scale exploration with lower calculation costs [13]. It produces location-sensitive data which very essential in analyzing thyroid nodules. The sub-bands for 1-level and 2-levels using two dimension DWT haar filters as a basis function wavelet decomposition are shown in Figure 1 [14].

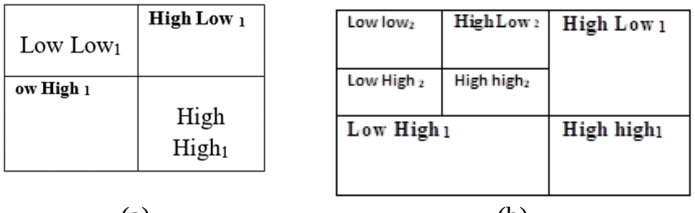

Figure 1. The DWT sub-band: (a) 1-level DWT and (b) 2-level DWT

3. DISCRETE COSINE TRANSFORM (DCT)

The DCT is a mathematical equation that takes a signal and transforms it from the spatial domain into the frequency domain, The DCT is the real part of the discrete fourier transform (DFT). The low frequency by in the left top corner, and when the frequency increased by zigzag order arrived at the right bottom corner [15]. An image of size (N*M) every pixel is denoted by p(x,y), The two-dimension DCT is used to transfer the image into P(u,v) DCT coeffic.

$$P(u,v) = \frac{1}{\sqrt{M+N}} C(u)C(v) \sum_{x=0}^{N}\sum_{y=0}^{M} p(i,j) Cos\left(\frac{(2x+1)2\pi}{2N}\right) Cos\left(\frac{(2y+1)2\pi}{2M}\right) \quad (1)$$

$$C(u), C(v) = \begin{cases} 1/\sqrt{2} & u,v = 0 \\ 1 & u,v \neq 0 \end{cases} \quad (2)$$

4. IMAGE GRADIENT

In image processing, the process of changing the values of color pixels is called color gradation. in measured, gradient of a two-dimension function at each point in the image p (x, y) produce two dimension vector with the values given by the derivatives in the vertical gv (i, j) and horizontal directions gv (x, y) at points in locations x row and y column [16]. The gradient vector values depend on pixels value and it distribution in the sub-block of size (3*3) [17], [18]. The gradient equation cconvertsimage pixels p (x, y) into two vectors gradient magnitude M (x, y) and gradient direction A (x,y).

$$g_v(x,y) = p(x-1,y+1) + 2p(x,y+1) + p(x+1,y+1) \quad (3)$$

$$-p(x-1,y-1) - 2p(x+1,y-1) - p(x+1,y-1) \quad (4)$$

$$g_h(x,y) = p(x-1,y-1) + 2p(x-1,y+1) + p(x-1,y+1) \quad (5)$$

$$-p(x+1,y-1) - 2p(x+1,y) - p(x+1,y+1) \quad (6)$$

$$M(x,y) = \sqrt{gv(x,y)^2 + gh(x,y)^2} \quad (7)$$

$$A(x,y) = tan^{-1}(gv(x,y)/gh(x,y)) \quad (8)$$

5. THE FIRST ORDER STATISTICAL METHOD

In skin cancer images many statistical methods have been used for the extraction features of data [17]. Among these, are color means variance skewness, and fourth momentum. It is very simple and is invariant to transformation coefficients information regarding an image, the statistic equation used in this work are [18]–[20].

a) Mean, the mean of coefficients X (i, j) of size M, N.

$$mean = \frac{\sum_{x=1}^{N}\sum_{y=1}^{M} p(x,v)}{N \times M} \quad (9)$$

b) Standard deviation

$$Std = \sqrt{\frac{\sum_{x=1}^{N}(p(x,y)-mean)^2}{N \times M}} \quad (10)$$

c) Skewness

$$Skewness = \frac{\sum_{x=1}^{N}\sum_{y=1}^{M} p(x,y)^3}{N \times M} \quad (11)$$

d) Fourth momentum

$$Fourth\ Momentum = \frac{\sum_{x=1}^{N}\sum_{y=1}^{M} p(x,y)^4}{N \times M} \quad (12)$$

e) Contrast [21], the segmented sub-region of size (n*n)

$$Contrast = \sum_{x=1}^{n}\sum_{y=1}^{n} \frac{p(x,y)-mean_{n*n}}{Std_{n*n}} \quad (13)$$

6. ANN NETWORKS

The ANN network comprises of three layers call input, output, and one or more hidden layer [21]. Training methods to build the networks accuracy depend on the values of the features like gradient or statistical methods (that used in this work) [22]. The network is built by calculated layers weight values, these values update by repetition of calculation to minimize the error between calculated output values and expected values. This problem is called the disappearing gradient [23], [24].

7. PROPOSED SKIN CANCER CLASSIFICATION METHOD

In this work, different skin image classification methods have been implemented. The proposed systems block diagram is shown in Figure 3.

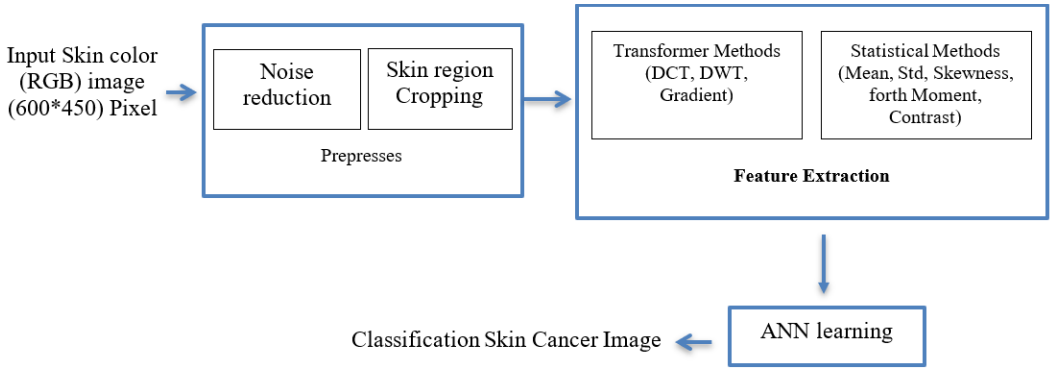

Figure 3. Block diagram of the skin cancer classification systems

8. THE PROPOSED SYSTEMS CONTAIN THREE CASCADE STAGES

8.1. Color image pre-proses

The preprocessing steps to extract cancer part from another skin part, namely i) Noise removal: Here unwanted pixels like hair are eliminated from the red, green, blue (RGB) images using median filters; ii) Cropping: Our area of interest is the cancer region. The white spaces surrounding cancer have been cropped; iii) Thinning: Cancer strokes are represented with minimum cross-sectional width by eliminating a few foreground pixels; and iv) Normalization: The RGB images are resized to three 128*128 pixels for cropping cancer regions only. The preprocessing step is shown in Figure 4. Figure 4(a) shows the cancer image, Figure 4(b) shows the image by median filter, Figure 4(c) shows thinning the cancer area, Figure 4(d) shows the sounding cancer region, Figure 4(e) shows the normalized the cropping image, and Figure 4(f) shows the normalized cancer region to 128*128 pixels.

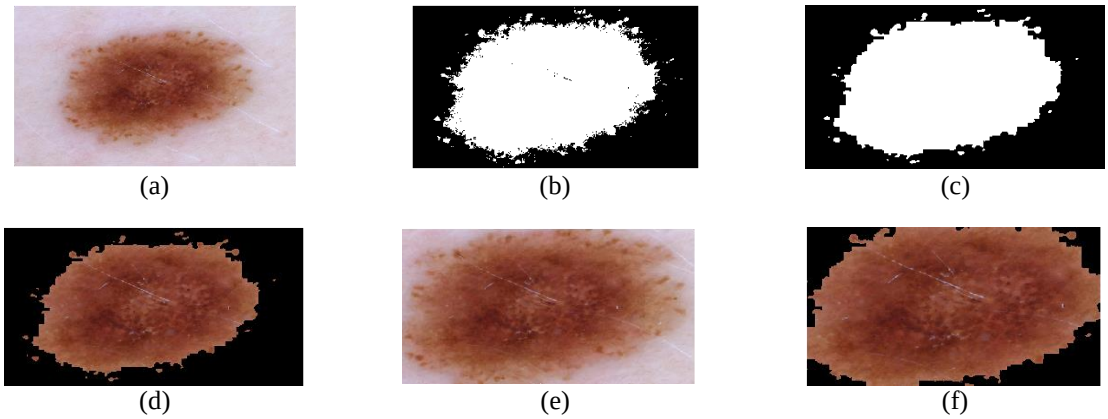

Figure 4. Propose system pre-processing: (a) cancer image, (b) filter image by median filter, (c) thinning the cancer area, (d) sounding cancer region, (e) Normalized the cropping image, and (f) normalized cancer region to 128*128 pixel

Algorithm (1): Preprocessing

Input: Skin Tumor Image File
Data Type: JPEG Image
Image Size: 450x600
Output**:** Preprocessing Color Image.
Segmented Image.
Reduce Size.
Begin
Step 1: Hair Removing Function
List1 ⟵ Read Skin Color image //ISIC 2018 dataset
List2 ⟵ Hair detection //use median filter
List3 ⟵ Remove Hair
List4 ⟵ Harmonic Inpainting Operation
Step 2: Segmentation and Resize Image Function
List1 ⟵ Read Image 450x600
List2 ⟵ Binarization
Step 3: Isolate the Tumor
List1 ⟵ Read Binary Image
List2 ⟵ Average Filter (5x5)
List3 ⟵ Full Space Average Filter (17x17)
List4 ⟵ Resize image (128*128)
End

8.2. Feature extraction

8.2.1. First step

The normalized cropped cancer region has been transformed into frequency domain. Three different transformations (DCT, DWT, and gradient explain above) have been used for (RGB) to extract the difference between the image's pixel and transform it. The proposed system divided the cropped image into sub-band (8*8), and the DCT for every sub-band in RGB images has been implemented to extract features from the neighborhood, this is shown in Figure 5. DCT for (RGB) Image is shown in Figure 5(a), The sub-block DCT for (RGB) image is shown in Figure 5(b). In Figure 6 shows the DWT coefficient for 1-level and 2-level. The 1-level DWT coefficients of R, G, and B image; and respectively shown in Figures 6(a), 6(b), 6(c); and the 2-level DWT of R, G, and B image, respectively shown in Figures 6(d), 6(e), 6(f). The magnitude of gradient transform for sub-band (8*8) in RGB images has been implemented as shown in Figure 7. For whole R image is shown in Figure 7(a) and for sub-block R image is shown in Figure 7(b).

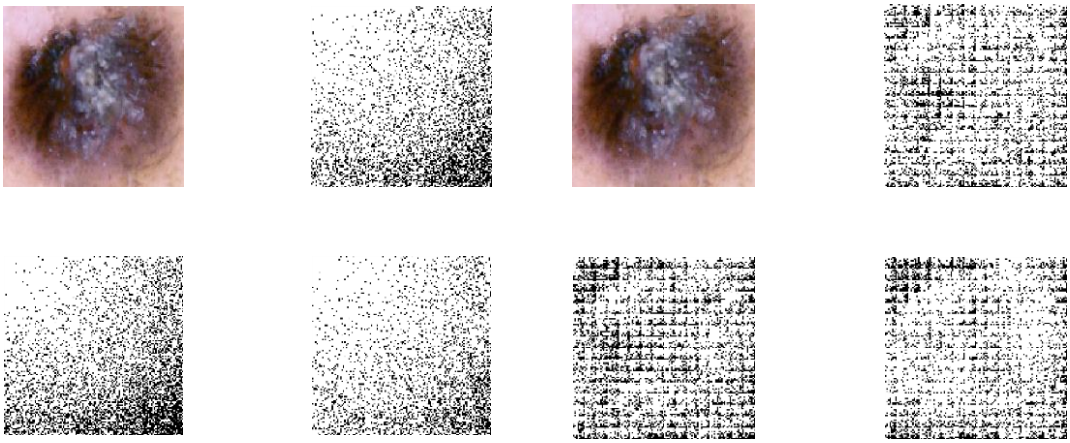

(a) (b)

Figure 5. The normalized cropped cancer region: (a) DCT for (RGB) image and (b) sub-block DCT for (RGB) image

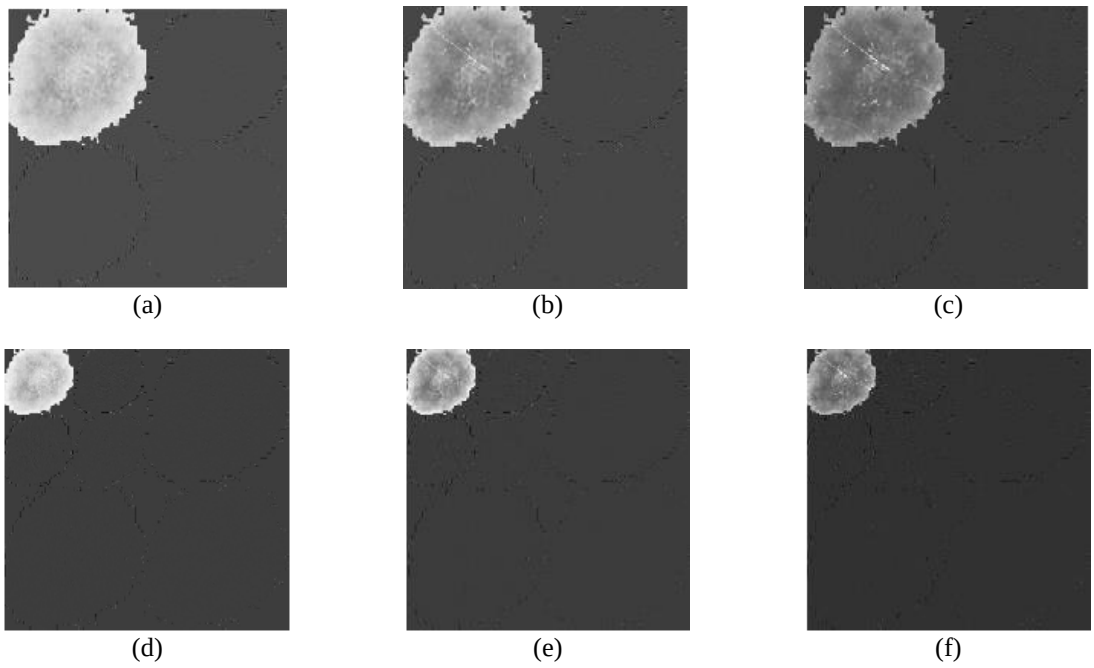

Figure 6. The DWT coefficient for 1-level and 2-level: (a) 1-level DWT coefficients of R, (b) 1-level DWT coefficients of G, (c) 1-level DWT coefficients of B, (d) 2-level DWT of R, (e) 2-level DWT of G, and (f) 2-level DWT of B

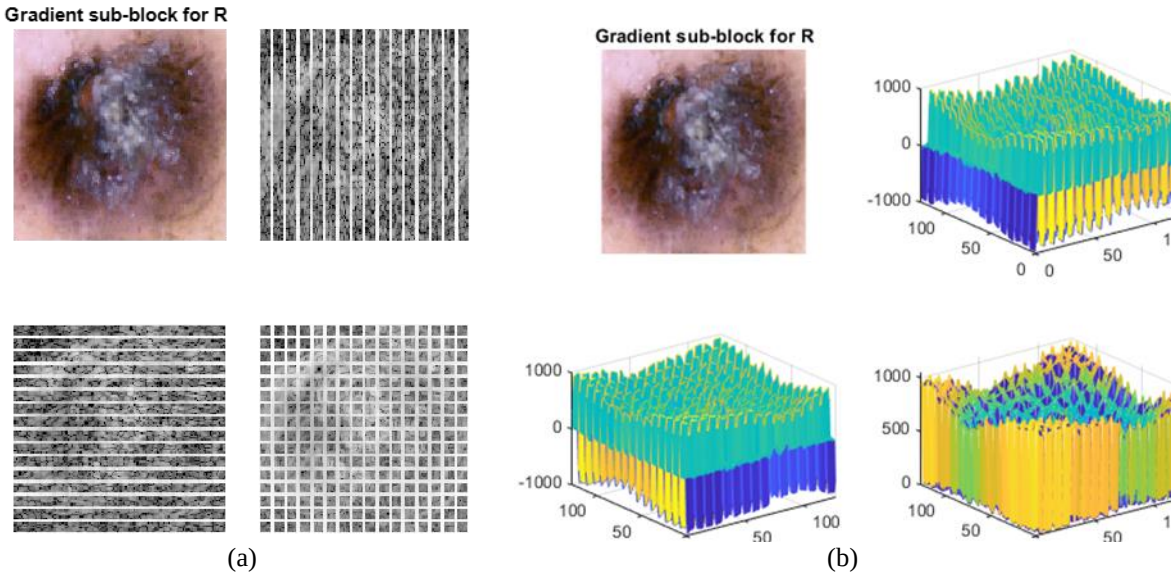

Figure 7. The magnitude of gradient transform to normalized cancer image (a) for whole R image and (b) for sub-block R image

8.2.2. Second step

The statistical method has been calculated (mean, std. dev., skewness, and fourth momentum) for RGB coefficient results in DCT, DWT, and gradient. When the contrast was calculated for cropped cancer image. This step helps to collect the result and minimized the size of data for learning. Figure 8 shows 1st order statistic feature for the DCT transform for the first 20 images, Figure 9 shows 1st order statistic feature for the DWT (Haar) 1'st level transform for the first 20 images, Figure 10 shows 2'ndst order statistic feature for the DWT (Haar) 2'st level transform for the first 20 images, Figure 11 shows 1st order statistic feature for the gradient transform for the first 20 images.

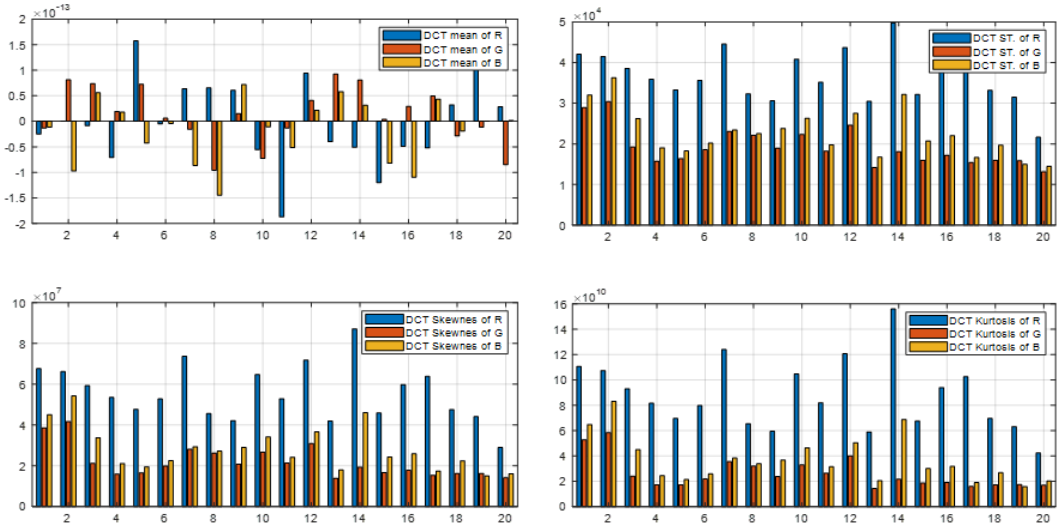

Figure 8. 1st order statistic feature for the DCT transform for the first 20 images

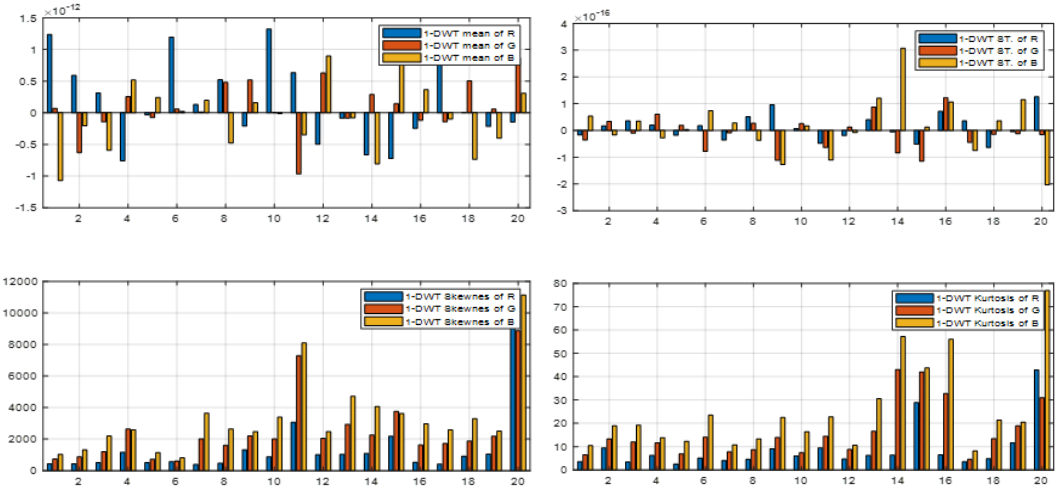

Figure 9. 1st order statistic feature for the first-level DWT transform for the first 20 images

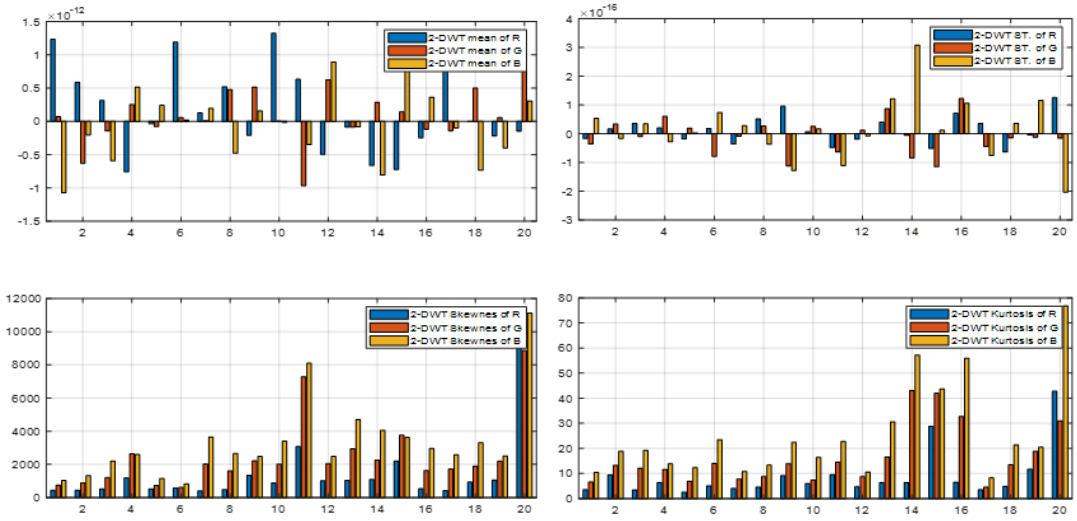

Figure 10. 1st order statistic feature for the second-level DWT

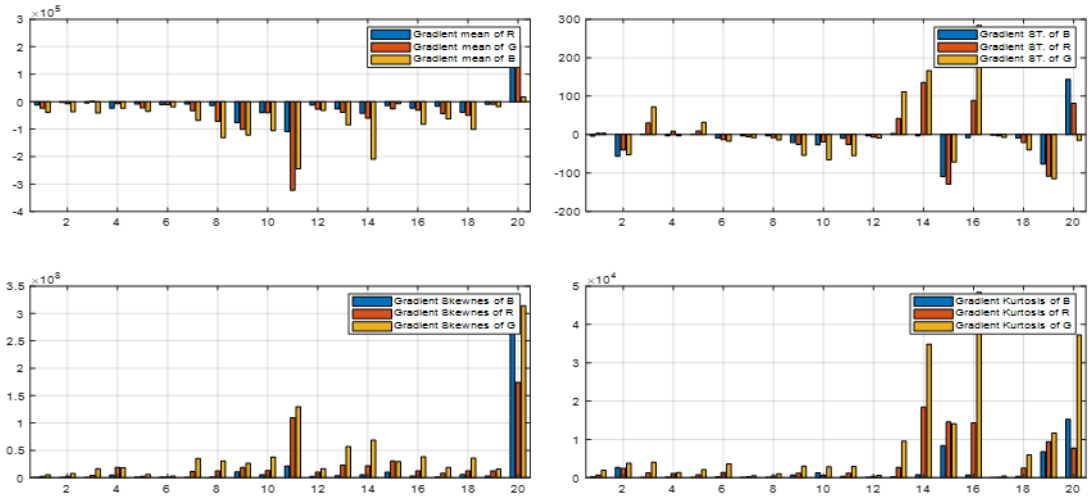

Figure 11. 1st order statistic feature for the gradient transform for the first 20 images

8.3. ANN network

The ANN (backpropagation method) has been used to build an artificial network for the classification of skin cancer. The ANN consists of two hidden layers every layer built from 20 nodes. The 200 iterations have been used to minimize the error. Figure 12 shows the diagram of DCT training, Figure 13 shows the diagram of gradient training, and Figure 14 shows the diagram of DWT (Haar) transform training.

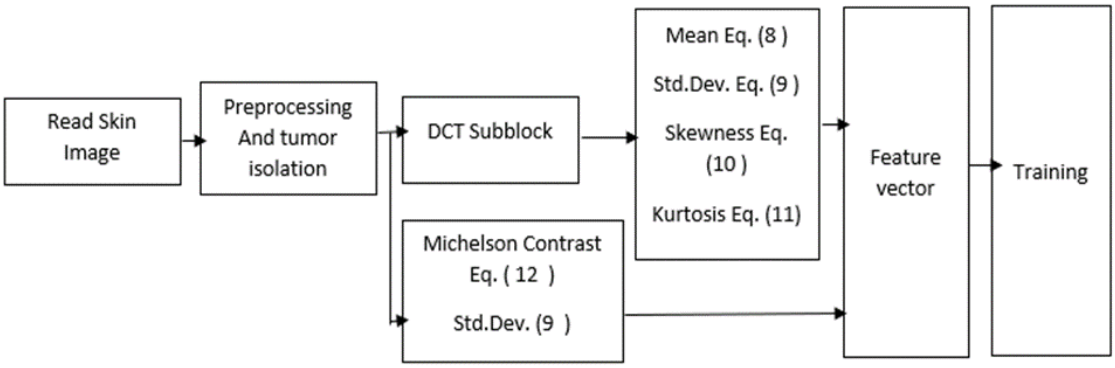

Figure 12. DCT feature training

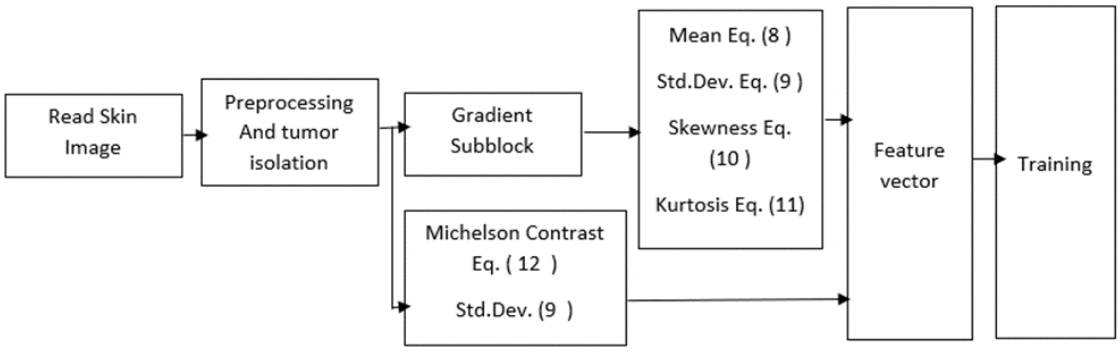

Figure 13. Gradient feature training

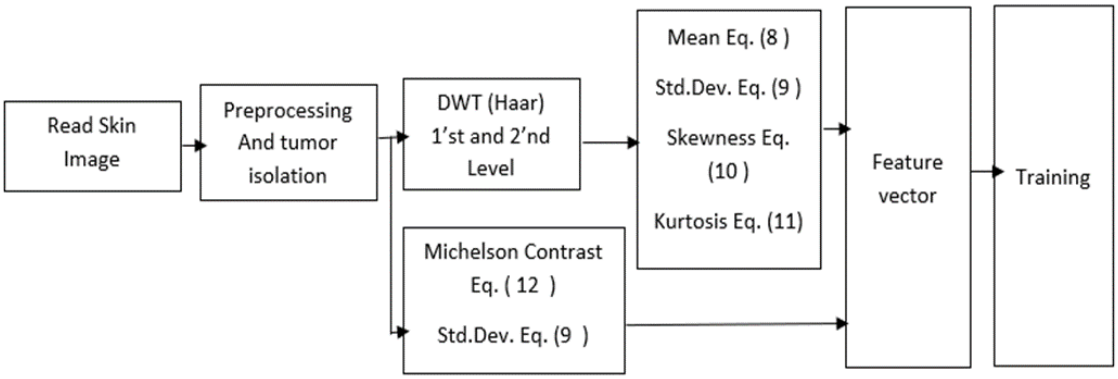

Figure 14. DWT feature training

9. RESULT OF PROPOSED SYSTEMS

In this work, the dataset of four different types of cancer images has been used, see Table 1. The three proposed method has been implemented to build three different classification ANN networks. The proposed method for feature extraction is implemented for sub-band DCT, DWT (1-level and 2-level), and sub-band gradient transform. In the second step, five statistic calculation has been applied to extract the minimum size of features (every color image have 3*5 = 15 feature values). The ANN used 70% of data for training and 25% of data for testing. The ANN train has a mean square error (MSE) as shown in Table 2. The confusing matrix used to implement three different skin cancer classification methods the testing results are shown in Table 3. The unbalance of skin cancer images in all types of the percentage of confusing matrix is shown in Table 4.

Table 1. Number of cancer image in dataset

No.	Cancer type	No. of images
1	Akiec	327
2	Bcc	513
3	Bki	1,098
4	Df	114

Table 2. The MSE of the ANN train for propose methods used

No.	Proposed method	MSE
1	Sub-band gradient methods	$12*10^{-4}$
2	Sub-band DCT methods	$7*10^{-4}$
3	1-level and 2-level DWT methods	$2*10^{-4}$

Table 3. The confusing matrix for proposed methods used

The sub-band gradient methods				
class	1	2	3	4
1	**117**	170	40	0
2	7	**391**	116	0
3	1	322	**756**	11
4	0	13	60	**42**
The sub-band DCT				
class	1	2	3	4
1	**228**	92	7	0
2	9	**432**	73	0
3	1	136	**939**	23
4	0	4	42	**69**
1-level, 2-level DWT				
class	1	2	3	4
1	**262**	62	3	0
2	18	**441**	55	0
3	0	96	**977**	26
4	0	4	35	**76**

Table 4. The percentage confusing matrix for proposed methods used

The sub-band gradient methods				
class	1	2	3	4
1	**35.779**	51.987	12.232	0
2	1.3618	**76.070**	22.568	0
3	0.091	29.299	**69.609**	1.001
4	0	11.304	52.174	**36.521**
The sub-band DCT				
class	1	2	3	4
1	**69.724**	28.134	2.141	0
2	1.7510	**84.047**	14.202	0
3	0.091	12.3758	**85.441**	2.093
4	0	3.4782	36.522	**60**
1-level, 2-level DWT				
class	1	2	3	4
1	**80.122**	18.960	0.917	0
2	3.502	**85.798**	10.701	0
3	0	8.735	**88.899**	2.366
4	0	3.478	30.435	**66.087**

10. CONCLUSION

The proposed methods have been established that a group of feature extraction methods with ANN built network can realize low-priced classification performance for skin cancer color image classification to skin cancer lesion. The ANN appears as highly preset and accurate. The inequality dataset with a big difference in total images for each class makes it complex to simplify the image features classification of the lesions. The result shown in Table 3 obtain that DWT methods give high perfection in cancer classification in a low number of cancer images. When sub-band DCT gives less ratio in error detect of on other types this falling the risk and expand the robustness of the method.

REFERENCES

[1] M. A. A. Milton, "Automated skin lesion classification using ensemble of deep neural networks in ISIC 2018: Skin lesion analysis towards melanoma detection challenge," Jan. 2019, [Online]. Available: http://arxiv.org/abs/1901.10802

[2] T. Y. Satheesha, D. Satyanarayana, M. N. Giriprasad, and K. N. Nagesh, "Detection of melanoma using distinct features," in *2016 3rd MEC International Conference on Big Data and Smart City (ICBDSC)*, Mar. 2016, pp. 1–6. doi: 10.1109/ICBDSC.2016.7460367.

[3] K. M. Hosny, M. A. Kassem, and M. M. Foaud, "Skin melanoma classification using deep convolutional neural networks," in *Deep Learning in Computer Vision*, Boca Raton, FL: CRC Press, 2020, pp. 291–314. doi: 10.1201/9781351003827-11.

[4] S. S. Han, M. S. Kim, W. Lim, G. H. Park, I. Park, and S. E. Chang, "Classification of the clinical images for benign and malignant cutaneous tumors using a deep learning algorithm," *Journal of Investigative Dermatology*, vol. 138, no. 7, pp. 1529–1538, Jul. 2018, doi: 10.1016/j.jid.2018.01.028.

[5] N. C. F. Codella *et al.*, "Skin lesion analysis toward melanoma detection: A challenge at the 2017 international symposium on biomedical imaging (ISBI), hosted by the international skin imaging collaboration (ISIC)," pp. 1–5, Oct. 2017, [Online]. Available: http://arxiv.org/abs/1710.05006

[6] R. S. S. Sundar and M. Vadivel, "Performance analysis of melanoma early detection using skin lession classification system," in *2016 International Conference on Circuit, Power and Computing Technologies (ICCPCT)*, Mar. 2016, pp. 1–5. doi: 10.1109/ICCPCT.2016.7530182.

[7] N. Gessert, M. Nielsen, M. Shaikh, R. Werner, and A. Schlaefer, "Skin lesion classification using ensembles of multi-resolution EfficientNets with meta data," *MethodsX*, vol. 7, pp. 1–8, 2020, doi: 10.1016/j.mex.2020.100864.

[8] D. S. M. Kumar, D. J. R. Kumar, and D. K. Gopalakrishnan, "Skin cancer diagnostic using machine learning techniques - shearlet transform and naïve Bayes classifier," *International Journal of Engineering and Advanced Technology*, vol. 9, no. 2, pp. 3478–3480, Dec. 2019, doi: 10.35940/ijeat.B4916.129219.

[9] M. Erode and T. Nadu, "MATLAB central program or color image segmentation." https://www.mathworks.com/matlabcentral/fileexchange/25257-color-image-segmentation (accessed Dec. 02, 2019).

[10] H. A. Haenssle *et al.*, "Man against machine: Diagnostic performance of a deep learning convolutional neural network for dermoscopic melanoma recognition in comparison to 58 dermatologists," *Annals of Oncology*, vol. 29, no. 8, pp. 1836–1842, Aug. 2018, doi: 10.1093/annonc/mdy166.

[11] C. Barata, M. E. Celebi, and J. S. Marques, "A survey of feature extraction in dermoscopy image analysis of skin cancer," *IEEE Journal of Biomedical and Health Informatics*, vol. 23, no. 3, pp. 1096–1109, May 2019, doi: 10.1109/JBHI.2018.2845939.

[12] M. K. Monika, N. A. Vignesh, C. U. Kumari, M. N. V. S. S. Kumar, and E. L. Lydia, "Skin cancer detection and classification using machine learning," *Materials Today: Proceedings*, vol. 33, pp. 4266–4270, 2020, doi: 10.1016/j.matpr.2020.07.366.

[13] A. Seal, D. Bhattacharjee, and M. Nasipuri, "Predictive and probabilistic model for cancer detection using computer tomography images," *Multimedia Tools and Applications*, vol. 77, no. 3, pp. 3991–4010, Feb. 2018, doi: 10.1007/s11042-017-4405-7.

[14] T. J. Brinker *et al.*, "Skin cancer classification using convolutional neural networks: Systematic review," *Journal of Medical Internet Research*, vol. 20, no. 10, pp. 1–8, Oct. 2018, doi: 10.2196/11936.

[15] H. Nahata and S. P. Singh, "Deep learning solutions for skin cancer detection and diagnosis," in *Machine Learning with Health Care Perspective*, Cham: Springer, 2020, pp. 159–182. doi: 10.1007/978-3-030-40850-3_8.

[16] M. A. M. Almeida and I. A. X. Santos, "Classification models for skin tumor detection using texture analysis in medical images," *Journal of Imaging*, vol. 6, no. 6, p. 51, Jun. 2020, doi: 10.3390/jimaging6060051.

[17] P. Tschandl, C. Rosendahl, and H. Kittler, "The HAM10000 dataset, a large collection of multi-source dermatoscopic images of common pigmented skin lesions," *Scientific Data*, vol. 5, no. 1, pp. 1–9, Dec. 2018, doi: 10.1038/sdata.2018.161.

[18] M. Combalia *et al.*, "BCN20000: Dermoscopic lesions in the wild," Aug. 2019, [Online]. Available: http://arxiv.org/abs/1908.02288

[19] R. M. Haralick, "Statistical and structural approaches to texture," *Proceedings of the IEEE*, vol. 67, no. 5, pp. 786–804, 1979, doi: 10.1109/PROC.1979.11328.

[20] N. B. Bahadure, A. K. Ray, and H. P. Thethi, "Image analysis for MRI based brain tumor detection and feature extraction using biologically inspired BWT and SVM," *International Journal of Biomedical Imaging*, vol. 2017, pp. 1–12, 2017, doi: 10.1155/2017/9749108.

[21] M. Abdel-Nasser, A. Moreno, and D. Puig, "Breast cancer detection in thermal infrared images using representation learning and texture analysis methods," *Electronics*, vol. 8, no. 1, pp. 1–18, Jan. 2019, doi: 10.3390/electronics8010100.

[22] S. Ayyachamy, "Registration based retrieval using texture measures," *Applied Medical Informatics*, vol. 37, no. 3, pp. 1–10, 2015.

[23] ISIC Challenge, "International skin imaging collaboration," 2019. https://challenge.isic-archive.com/landing/2019/ (accessed Dec. 02, 2019).

[24] T. J. Brinker *et al.*, "Deep learning outperformed 136 of 157 dermatologists in a head-to-head dermoscopic melanoma image classification task," *European Journal of Cancer*, vol. 113, pp. 47–54, May 2019, doi: 10.1016/j.ejca.2019.04.001.